GEOLOGY | THE GEOLOGICAL SOCIETY OF AMERICA®

https://doi.org/10.1130/G54477.1

Manuscript received 31 January 2026
Revised manuscript received 27 March 2026
Manuscript accepted 8 April 2026

Published online 20 April 2026

Controls on canyon formation along mud-rich continental margins

Qiliang Sun[1,2], Vittorio Maselli[3,4,*], Xingxing Wang[1], Yunlong He[1], Dave Reynolds[4], and Andrea Fildani[5,6]
[1]Hubei Key Laboratory of Marine Geological Resources, China University of Geosciences, Wuhan 430074, China
[2]Laboratory for Marine Mineral Resources, Qingdao Marine Science and Technology Center, Qingdao 266005, China
[3]Department of Chemical and Geological Sciences, University of Modena and Reggio Emilia, Modena 41125, Italy
[4]Department of Earth and Environmental Sciences, Dalhousie University, Halifax, B3H 4R2 Nova Scotia, Canada
[5]Department of Earth, Environmental and Resources Sciences, University of Naples Federico II, Naples 80126, Italy
[6]Department of Earth and Planetary Sciences, Stanford University, Stanford, California 94305, USA

ABSTRACT

Submarine canyons are conduits for transferring land-derived materials from continents to the deep ocean. Regional and global studies show that canyon occurrence correlates positively with seafloor gradient and supply of coarse sediment, yet the processes governing their initiation remain elusive. Here, we investigated the northern South China Sea (SCS) where the spatial variations in fine-grained input from the Red River, delivered to the shelf and slope by buoyant sediment plumes, exert a critical control on canyon development. From SW to NE, the northern SCS transitions from an aggradational-progradational margin with a smooth seafloor devoid of canyons to a purely aggradational margin deeply incised by canyons, gullies, and landslide scars. Seismic and well data show mass-transport deposits are pervasive across the margin, even in the western sector where canyon headscarps are absent at the seafloor. We posit that where the accumulation rate of fine-grained sediment at the shelf edge exceeds tectonic subsidence, rapid mud deposition heals landslide scars and mantles the seafloor, thereby inhibiting canyon formation. By contrast, where sediment supply is lower and balances tectonic subsidence, steeper gradients favor erosion by gravity flows and canyon incision. These results highlight the need to consider sediment supply, caliber, and lateral advection by coastal currents together with slope gradient when predicting canyon distribution.

1. INTRODUCTION

Submarine canyons are deep, V- and box-shaped incisions cut into bedrock and sediment across continental shelves and slopes that connect continental landmasses to the abyssal ocean. Their origin and evolution remain debated, even as advances in deep-water remote sensing, bottom and suspended sediment sampling, and numerical modeling continue to refine our understanding (Talling et al., 2015; Bernhardt and Schwanghart, 2025). Current models for canyon initiation emphasize fluvial incision during relative sea-level fall below the shelf edge or canyon-head development via submarine landslides and retrogressive headscarp migration (Farre et al., 1983; Posamentier et al., 1988; Green and Uken, 2008), especially on steeper slopes (Bernhardt and Schwanghart, 2025). Sediment-gravity flows, including erosive turbidity currents, have likewise been invoked for channel inception and the establishment of long-lived conduits to deep water (Pratson and Coakley, 1996; Fildani et al., 2013; Covault et al., 2014). The highest likelihood of canyon occurrence has also been observed where rivers supply abundant coarse, indurated bedrock clasts capable of enhancing seabed erosion (Smith et al., 2017, 2018).

By contrast, the role of fine-grained sediments and oceanographic processes in canyon formation has so far been overlooked. This is notable because many mud-rich continental margins fed laterally by buoyant river plumes do not exhibit pervasive canyon incisions. This observation raises the question: In addition to seafloor gradient, do caliber, flux, and routing of sediment influence whether submarine canyons can initiate and persist? More specifically, does abundant fine-grained sediment delivered to the continental margin hamper submarine canyon formation?

Here, we investigated the northern South China Sea (SCS; Fig. 1), a subsiding margin characterized by substantial along-shelf sediment transport and spatially variable canyon development (Li et al., 2022). We show how rapid sediment accumulation in mud-rich slope clinoforms can blanket the seafloor and smooth antecedent relief, thereby inhibiting the transformation of landslide headscarps or slope gullies into deeply incised submarine canyons.

2. GEOLOGICAL SETTING

Rifting of the northern SCS began in the late Paleogene (Nagel et al., 2015), with margin outbuilding developing since the early Miocene (Xie et al., 2008). The basin experienced three phases of tectonic subsidence (Zhao et al., 2018), the last of which started ca. 5.5 Ma with mean subsidence rate changing from 80–100 to <10 m/m.y. moving from SW to NE along the upper slope region (Section SI-1 in the Supplemental Material[1]).

The sedimentary succession consists of shelf-margin clinothem sets, bounded by five regionally extensive seismic horizons, constrained and dated in previous studies (T40 at ca. 10.5 Ma, T30 at ca. 5.5 Ma, T29 at ca. 4.2 Ma, T27 at ca. 2.7 Ma, and T20 at ca. 1.8 Ma; Supplemental Material Section SI-2; Xie et al., 2008; Zhao et al., 2019; Chen et al., 2020).

3. DATASET AND METHODS

Multibeam bathymetric data, with a lateral and vertical resolution of ~100 m and 1–6 m, respectively, cover an area of 11,120 km^2 (see additional information in Supplemental Material S2). 2-D seismic reflection profiles, zero-phase and displayed with Society of Exploration Geophysicists normal polarity, were poststack time migrated with a dominant frequency of ~40–45 Hz, which resulted in a vertical resolution of ~10 m given an average

Vittorio Maselli https://orcid.org/0000-0001-7301-0769
*vmaselli@unimore.it

[1]Supplemental Material. Text Sections SI-1 to SI-5, references, and Figures SI-1 to SI-5. Please visit https://doi.org/10.1130/GEOL.S.31975143 to access the supplemental material; contact editing@geosociety.org with any questions.

CITATION: Sun, Q., et al., 2026, Controls on canyon formation along mud-rich continental margins: Geology, v. XX, p. , https://doi.org/10.1130/G54477.1

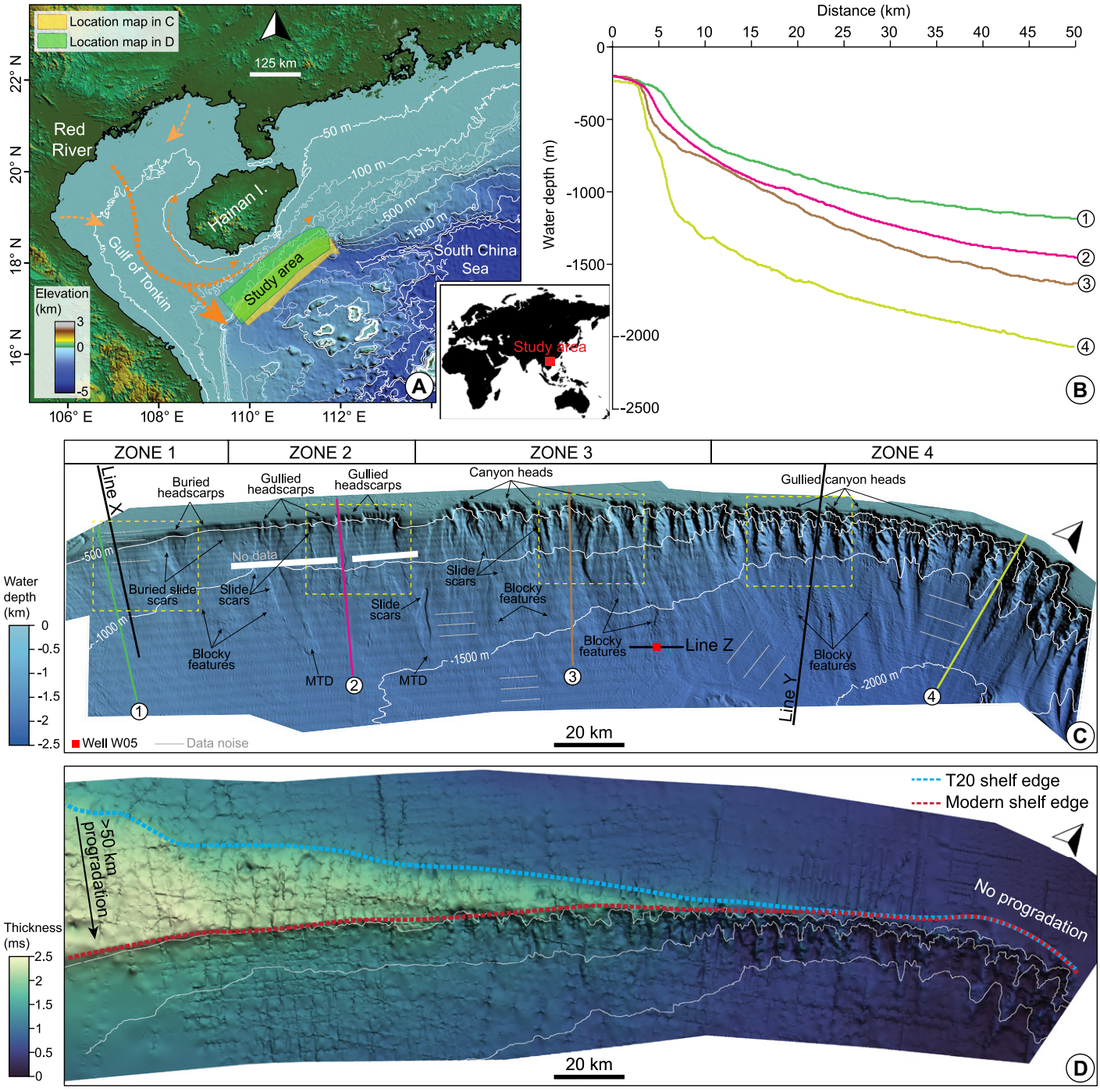

Figure 1. (A) Map of northern South China Sea (SCS) with direction of surface transport (orange arrows). Green and yellow areas are locations of maps in C and D, respectively. I.—Island. (B) Bathymetric profiles located in map C (colored lines 1–4). (C) Seafloor bathymetry with main depositional/erosional features noted. Red square shows location of well W05; black lines are seismic profiles in Figure 3; dashed yellow squares are maps reported in Figure 2 (maps A to D, from left to right); short gray lines indicate direction of data noise or artifacts in multibeam bathymetric data. MTD—mass-transport deposit. (D) Isochrone map between seafloor and horizon T20 (1.8 Ma); red and cyan dashed lines indicate positions of modern and T20 shelf-edge shorelines, respectively.

velocity of 1800 m/s. Lithology and logs from well W05 are from Kuang et al. (2023).

4. RESULTS

4.1. Seafloor Morphology

We divided a 350-km-long stretch of the northern SCS slope into four zones based on morphological characteristics (Fig. 1).

Zone 1 (southwesternmost area; Fig. 1) is characterized by a <3° slope at its upper, most inclined sector (Fig. 1B), where the seafloor lacks obvious canyon incisions or slide scars (Fig. 1C). Overall, the slope morphology is smooth (Figs. 1C and 2A), showing only subtle relief that may correspond to buried mass-transport deposits (MTDs) and to shallow gullies or weakly channelized sediments. Toward the northeast, the shelf edge reaches slopes of up to ~5°–8°. We identified two smooth escarpments, up to 8 km wide, on the southwestern side (Figs. 1C and 2A). Their gentle morphologies suggest they may represent buried slide headscarps, as also indicated by the blocky features observed basinward.

In zone 2, the upper slope shows 2–4-km-wide and 10–15-km-long incisions, with relief ranging from 40 to 120 m, and small-scale gullies running roughly perpendicular to the shelf break (Figs. 1C and 2B). Downslope, lobate and blocky deposits, with signs of channel reworking, are present, implying that the shelf-edge incisions started with landslide headscarps that were later modified by turbidity currents.

In zones 3 and 4, the shelf edge is cut by several well-defined canyons, 15–30 km long and 5–10 km wide, with ~8°–15° canyon wall gradients (Figs. 1B, 1C, 2C, and 2D). In zone 3, the depth of incision is between 100 and 250 m, and the canyon heads lack or show poorly developed gullies (Fig. 2C). In zone 4, the incisions are more pronounced, reaching depths up to 450 m, the amphitheater rims are reworked by well-developed gullies, and the interchannel areas also show signs of failures by lateral erosion (Fig. 2D). Basinward, remnants of buried MTDs appear as blocky features.

4.2. Stratigraphy

Post-Miocene sediments along the slope form a wedge that is thickest in zone 1 and thins northeastward toward zone 4 (Fig. 1D; Supplemental Material Section SI-3), consistent with an along-strike decrease in sediment accumulation from ~691 to ~216 m/m.y. over the past ~1.8 m.y. (Xie et al., 2008).

Seismic line X across zone 1 (Fig. 3) exhibits strongly aggradational-progradational clinoforms formed since the mid-Miocene (T40), characterized by low-amplitude sigmoidal units consisting mainly of green mudstones with <10% sand (Supplemental Material Section SI-3; Chen et al., 2020). Along the slope, reflection packages show mid- to low-amplitude facies interbedded with more chaotic reflections, likely representing alternating turbidites, hemipelagites, and MTDs, with the latter dominating.

Frequent shelf-edge collapse is evidenced by erosional truncations and MTDs, best imaged in the youngest slope margin clinoforms (Fig. 3). Over the past 1.8 m.y. (T20), the shelf has aggraded by >2000 ms and prograded >50 km (Fig. 1D).

Line Y shows mainly aggrading clinoforms in the region dominated by slope canyons at the modern seafloor, with <2 km progradation after T20. Muddy MTDs are widespread across the margin and form much of the deep-water stratigraphy above T30 (Cheng et al., 2025), especially after T20. Well W05, cored at 1785 m water depth in zone 3, contains stacked, muddy MTDs interbedded with hemipelagites and a few sandy turbidite beds (Fig. 3; Kuang et al., 2023).

5. DISCUSSION

5.1. Lateral Advection of Fine-Grained Sediments in Canyon Formation

Over the past 1.8 m.y., Red River sediment supply (Ss) in the northwestern SCS (zone 1) outpaced tectonic subsidence (Ts) of 80–100 m/m.y., forming sigmoidal clinothem sets with strong aggradation, progradation, and shelf-edge migration of up to 250–300 m/10 k.y. Conversely, in zone 4, sediment input only balanced subsidence rates of <10 m/m.y., yielding mainly aggradational clinoforms. Seismic and well data reveal that the post-T20 slope succession (Fig. 3), and likely older intervals, is pervasively composed of muddy MTDs (Cheng et al., 2025). These MTDs extend beneath zone 1, where the seafloor is nearly featureless at ~100 m multibeam resolution, northeastward to zone 4, where lower sediment supply coincides with a shelf edge incised by gullies, canyons, and landslide scours. These observations indicate that where fine-grained sediment accumulation in slope-margin clinoforms outpaces subsidence, evacuation zones at landslide headscarps are rapidly infilled, preventing upslope retreat and limiting incision, thereby promoting rapid autogenic healing of the margin. Conversely, where sediment supply is reduced, underfilled landslide escarpments can funnel and accelerate sediment-laden flows across the shelf break, enhancing erosion and gully development (Kneller, 2003; Lai et al., 2016) and seeding canyon-head initiation.

As discussed in Zhao et al. (2019), sediments in the northern SCS are mainly supplied by the (paleo-) Red River and dispersed to the NE by buoyant plumes advected by coastal currents, with only minor contributions from Hainan Island and Vietnamese rivers (see Supplemental Material Section SI-4). Over multiple sea-level cycles, these mud-rich sediments accumulate in kilometer-high clinoforms that develop asymmetrically from SW to NE in response to shifts in sediment-dispersal pathways and depocenters (Zhao et al., 2019). This interpretation is consistent with: (1) modern sediment budgets from the Gulf of Tonkin, indicating that ~30% of the total Red River sediment load (110–130 Mt/yr, of which ~90 Mt/yr is transported as suspended load; Milliman and Meade, 1983; Dang et al., 2010) is transferred to the deep sea (Anh and Van Quan, 2020); and (2) the thickness and provenance of slope deposits (Supplemental Material Section SI-3; Wang et al., 2014; Wan et al., 2015).

At the global scale, Bernhardt and Schwanghart (2025) identified slope gradient as a first-order control on canyon density. The northern SCS generally supports this model, with higher canyon densities where slopes are steeper. Our results, however, underscore the importance of sediment grain size, sediment supply, and along-strike routing, factors not explicitly represented in their predictor set. Where Ss/Ts >1, low-gradient slopes develop as a result of sediment dynamics and composition, with muddy systems yielding gentler slopes than coarse-

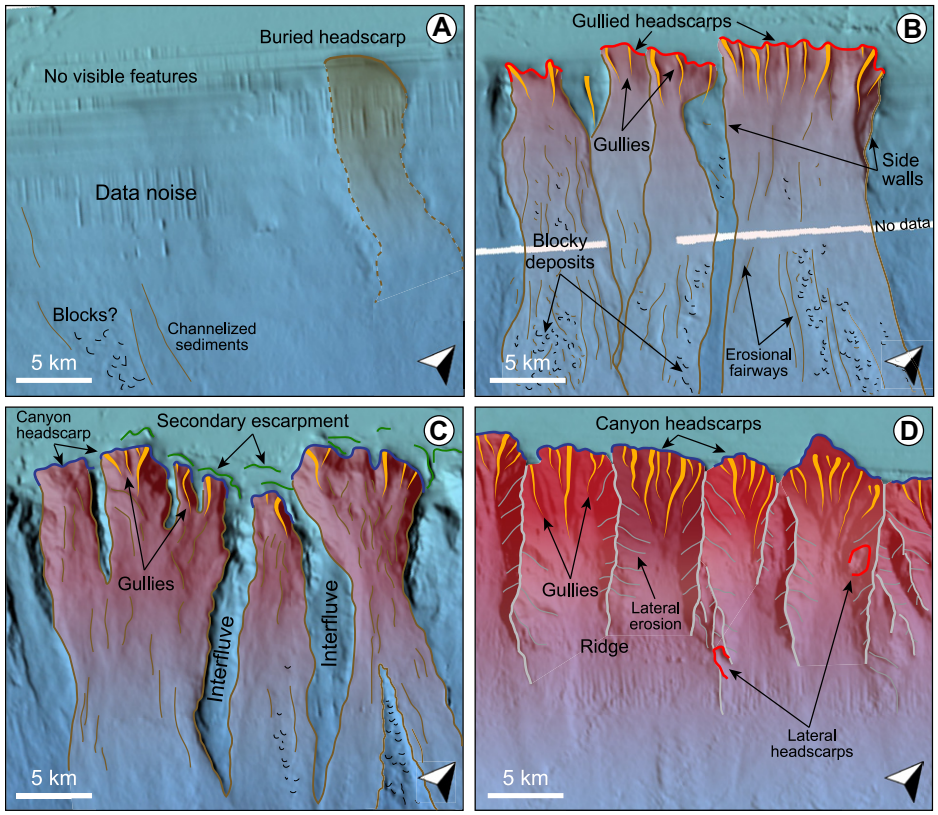

Figure 2. Close-up views of seafloor in zones 1–4 (maps A to D, respectively). Locations are shown in Figure 1C. Decreasing opacity of transparent red color indicates increasing seafloor slope and water depth.

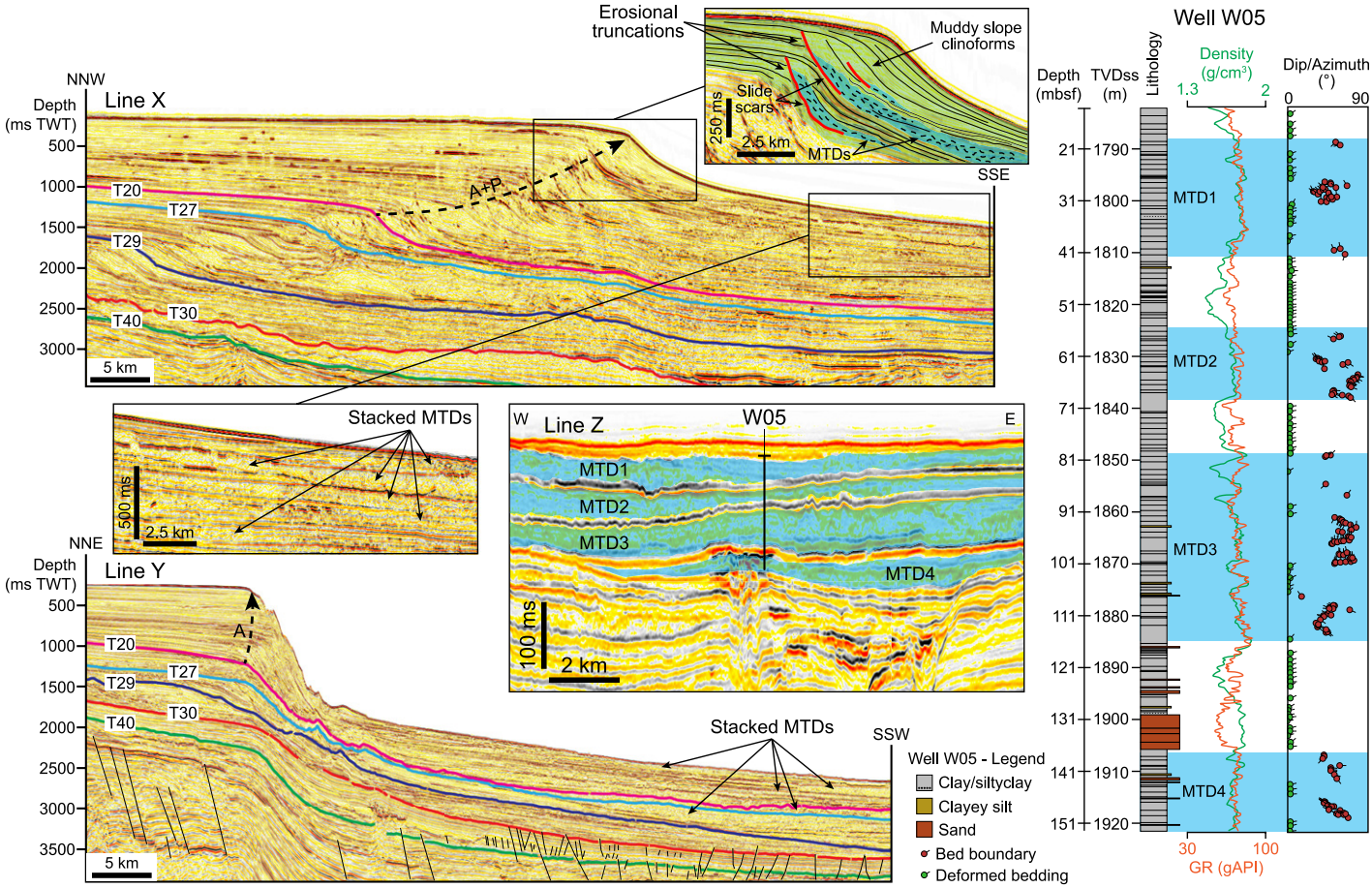

Figure 3. (Left) Seismic profiles with dated horizons crossing aggradational to progradational (A + P) clinoforms in zone 1 (line X) and aggradational (A) clinoforms of zone 4 (line Y). Line Z crosses well W05 with interpreted mass-transport deposits (MTDs) in blue. TWT—two-way traveltime. (Right) Stratigraphy of well W05 with density and gamma gay (GR) profiles and dip/azimuth data. Blue areas mark MTDs; mbsf—meters below seafloor; TVDss—true vertical depth subsea.

grained ones (Pirmez et al., 1998; Kostic et al., 2002). Conversely, tectonic tilting generates steeper gradients. This relationship is evident in the northern SCS: Zone 1 (Ss/Ts ≫1) has an ~1° clinoform slope (between 250 and 1250 m water depth) and predominantly depositional flows, whereas zone 4, where sediment supply is lower and tectonic subsidence dominates despite being weaker than in zone 1, has a steeper ~5.2° slope and predominantly erosional flows.

Margin evolution and canyon initiation may differ between systems in which feeder rivers are dominated by suspended load, so that sediment delivered to the margin is mainly fine grained and readily redistributed by coastal currents, and systems in which bed load is higher or where canyons incise the shelf to the river mouth, allowing canyon activity to persist through sea-level highstands and lowstands. The Congo River to canyon system is often cited as an example of the latter situation, where efficient river mouth–canyon head coupling promotes direct sediment capture and sustained canyon-fan growth; early work further inferred that a large fraction of the river's total sediment load was transported as bed load (~70%–80% of 160–180 Mt/yr; Peters, 1978). In contrast, although the Red River delivered a comparable total sediment flux prior to major damming (Milliman and Meade, 1983; Dang et al., 2010), it represents a fundamentally different sediment-routing system in which the load is dominated by fine-grained suspended sediment redistributed across the shelf and upper slope by coastal currents (van Maren and Hoekstra, 2005). A direct link between abundant, coarse, river-fed sediments and a high likelihood of canyon occurrence and development has also been identified along the western North American margin (Smith et al., 2017, 2018), further highlighting the importance of sediment supply and grain size. Together, these examples suggest that sediment can either promote canyon incision, especially if coarse, or inhibit it by blanketing the seabed and smoothing relief, especially if fine grained. This dual role seems to align with fluvial bedrock-incision models involving saltating bed load, which show that incision is controlled by both sediment supply relative to transport capacity and grain size, reflecting the trade-off between the availability of abrasive particles and bed cover by excess sediment (Sklar and Dietrich, 2004). Although developed for subaerial bedrock incision, similar approaches with the necessary adjustments may help geoscientists understand how grain size and sediment supply influence submarine canyon initiation.

5.2. Application to Other Margins

Similar conditions to those in the northwestern SCS occur in other modern and ancient basins. Along the eastern Mediterranean margin, down current of the Nile Delta (see Supplemental Material Section SI-5), slope failures are widespread in the mud-dominated sector offshore Israel, which is influenced by alongstrike dispersal of fine-grained sediment from the Nile plume (Stanley, 1989), whereas canyons become progressively more common offshore Lebanon, as the influence of Nile-derived mud diminishes. Even though local controls, such as strike-slip deformation, may also contribute to such along-margin variability, the first-order similarity with the northern SCS is notable. An ancient analogue is provided by Eocene clinothem complexes in the Central Basin of Spitsbergen (Plink-Björklund and Steel, 2005),

where outcrop-scale shelf-margin transects show enhanced mud-prone deposition at the shelf edge damping upper slope incision, limiting channel formation, and trapping sediment at the shelf margin, thereby suppressing sand export to basin-floor fans, as observed in the post-Miocene northern SCS.

6. CONCLUSIONS

This study shows that high rates of mud accumulation at the shelf edge, supplied from rivers and transported by coastal currents, can promote repeated slope failure while rapidly infilling incipient failure scars, thereby inhibiting canyon initiation. As a result, slope stratigraphy becomes dominated by muddy MTDs overlain by rapidly deposited fine-grained sediment that mantles the seabed. Classic models of canyon formation typically view the system in two dimensions along a river-to-canyon transect and are commonly derived from coarse-grained settings. We expand this view by showing that continental margin evolution and canyon incision are inherently three dimensional and strongly influenced by the volume and caliber of river-fed sediments, as well as by coastal dynamics and basin processes.

ACKNOWLEDGMENTS

This work was supported by the National Natural Science Foundation of China (grant/award number: 42222607). We thank the editor, and we are grateful to Ron Steel, Peter Talling, and Wolfgang Schwanghart for their insightful comments and stimulating discussion.

REFERENCES CITED

Anh, N.N., and Van Quan, N., 2020, A tentative sediment budget for the Red River subaqueous delta in the Gulf of Tonkin: A synthesis of existing data: Regional Studies in Marine Science, v. 34, https://doi.org/10.1016/j.rsma.2019.101005.

Bernhardt, A., and Schwanghart, W., 2025, Seafloor slopes control submarine canyon distribution: A global analysis: Science Advances, v. 11, https://doi.org/10.1126/sciadv.adv3942.

Chen, S., Steel, R., Wang, H., Zhao, R., and Olariu, C., 2020, Clinoform growth and sediment flux into late Cenozoic Qiongdongnan shelf margin, South China Sea: Basin Research, v. 32, p. 302–319, https://doi.org/10.1111/bre.12400.

Cheng, C., Jiang, T., Kuang, Z., Ren, J., Chen, Z., Zhao, X., Rahman, M.U., and Ning, F., 2025, A complete and continuous core record of deep-water mass transport deposits: Frontiers in Marine Science, v. 12, https://doi.org/10.3389/fmars.2025.1599494.

Covault, J.A., Kostic, S., Paull, C.K., Ryan, H.F., and Fildani, A., 2014, Submarine channel initiation, filling and maintenance from sea-floor geomorphology and morphodynamic modelling of cyclic steps: Sedimentology, v. 61, p. 1031–1054, https://doi.org/10.1111/sed.12084.

Dang, T.H., Coynel, A., Orange, D., Blanc, G., Etcheber, H., and Le, L.A., 2010, Long-term monitoring (1960–2008) of the river-sediment transport in the Red River watershed (Vietnam): Temporal variability and dam-reservoir impact: Science of the Total Environment, v. 408, p. 4654–4664, https://doi.org/10.1016/j.scitotenv.2010.07.007.

Farre, J.A., McGregor, B.A., Ryan, W.B.F., and Robb, J.M., 1983, Breaching the shelf break: Passage from youthful to mature phase in submarine canyon evolution, *in* Stanley, D.J., and Moore, G.T., eds., The Shelf-Break: Critical Interface on Continental Margins: SEPM (Society for Economic Paleontologists and Mineralogists [now Society for Sedimentary Geology]) Special Publication 33, p. 25–39.

Fildani, A., Hubbard, S.M., Covault, J.A., Maier, K.L., Romans, B.W., Traer, M., and Rowland, J.C., 2013, Erosion at inception of deep-sea channels: Marine and Petroleum Geology, v. 41, p. 48–61, https://doi.org/10.1016/j.marpetgeo.2012.03.006.

Green, A., and Uken, R., 2008, Submarine landsliding and canyon evolution on the northern KwaZulu-Natal continental shelf, South Africa, SW Indian Ocean: Marine Geology, v. 254, p. 152–170, https://doi.org/10.1016/j.margeo.2008.06.001.

Kneller, B., 2003, The influence of flow parameters on turbidite slope channel architecture: Marine and Petroleum Geology, v. 20, p. 901–910, https://doi.org/10.1016/j.marpetgeo.2003.03.001.

Kostic, S., Parker, G., and Marr, J.G., 2002, Role of turbidity currents in setting the foreset slope of clinoforms prograding into standing fresh water: Journal of Sedimentary Research, v. 72, p. 353–362, https://doi.org/10.1306/081501720353.

Kuang, Z., Cook, A., Ren, J., Deng, W., Cao, Y., and Cai, H., 2023, A flat-lying transitional free gas to gas to gas hydrate system in a sand layer in the Qiongdongnan Basin of the South China Sea: Geophysical Research Letters, v. 50, https://doi.org/10.1029/2023GL105744.

Lai, S.Y.J., Gerber, T.P., and Amblas, D., 2016, An experimental approach to submarine canyon evolution: Geophysical Research Letters, v. 43, p. 2741–2747, https://doi.org/10.1002/2015GL067376.

Li, S., Alves, T.M., Li, W., Wang, X., Rebesco, M., Li, J., Zhao, F., Yu, K., and Wu, S., 2022, Morphology and evolution of submarine canyons on the northwest South China Sea margin: Marine Geology, v. 443, https://doi.org/10.1016/j.margeo.2021.106695.

Milliman, J.D., and Meade, R.H., 1983, World-wide delivery of river sediment to the oceans: The Journal of Geology, v. 91, p. 1–21, https://doi.org/10.1086/628741.

Nagel, S., Granjeon, D., Willett, S., and Lin, A.T., 2015, Stratigraphic modeling of the Western Taiwan foreland basin: Sediment flux from a growing mountain range and tectonic implications: Marine and Petroleum Geology, v. 98, p. 331–347, https://doi.org/10.1016/j.marpetgeo.2018.05.034.

Peters, J.J., 1978, Discharge and sand transport in the braided zone of the Zaire Estuary: Netherlands Journal of Sea Research, v. 12, p. 273–292, https://doi.org/10.1016/0077-7579(78)90031-5.

Pirmez, C., Pratson, L.F., and Steckler, M.S., 1998, Clinoform development by advection-diffusion of suspended sediment: Modeling and comparison to natural systems: Journal of Geophysical Research, v. 103, p. 24,141–24,157, https://doi.org/10.1029/98JB01516.

Plink-Björklund, P., and Steel, R., 2005, Deltas on falling-stage and lowstand shelf margins, the Eocene Central Basin of Spitsbergen: Importance of sediment supply, *in* Giosan, L., and Bhattacharya, J.P., eds., River Deltas: Concepts, Models, and Examples: SEPM (Society for Sedimentary Geology) Special Publication 83, p. 179–206, https://doi.org/10.2110/pec.05.83.0179.

Posamentier, H.W., Jervey, M.T., and Vail, E.R., 1988, Eustatic controls on clastic deposition, I. Conceptual framework, *in* Wilgus, C.K., Hastings, B.S., Kendall, C.G.St.C., Posamentier, H.W., Ross, C.A., and Van Wagoner, J.C., eds., Sea-Level Changes: An Integrated Approach: SEPM (Society of Economic Paleontologists and Mineralogists) Special Publication 42, p. 109–124, https://doi.org/10.2110/pec.88.01.0109.

Pratson, L.F., and Coakley, B.J., 1996, A model for the headward erosion of submarine canyons induced by downslope-eroding sediment flows: Geological Society of America Bulletin, v. 108, p. 225–234, https://doi.org/10.1130/0016-7606(1996)108<0225:AMFTHE>2.3.CO;2.

Sklar, L.S., and Dietrich, W.E., 2004, A mechanistic model for river incision into bedrock by saltating bed load: Water Resources Research, v. 40, W06301, https://doi.org/10.1029/2003WR002496.

Smith, M.E., Finnegan, N.J., Mueller, E.R., and Best, R.J., 2017, Durable terrestrial bedrock predicts submarine canyon formation: Geophysical Research Letters, v. 44, p. 10,332–10,340, https://doi.org/10.1002/2017GL075139.

Smith, M.E., Werner, S.H., Buscombe, D., Finnegan, N.J., Sumner, E.J., and Mueller, E.R., 2018, Seeking the shore: Evidence for active submarine canyon head incision due to coarse sediment supply and focusing of wave energy: Geophysical Research Letters, v. 45, p. 12,403–12,413, https://doi.org/10.1029/2018GL080396.

Stanley, D.J., 1989, Sediment transport on the coast and shelf between the Nile Delta and Israeli margin as determined by heavy minerals: Journal of Coastal Research, v. 5, p. 813–828, https://www.jstor.org/stable/4297616.

Talling, P.J., et al., 2015, Key future directions for research on turbidity currents and their deposits: Journal of Sedimentary Research, v. 85, p. 153–169, https://doi.org/10.2110/jsr.2015.03.

van Maren, D.S., and Hoekstra, P., 2005, Dispersal of suspended sediments in the turbid and highly stratified Red River plume: Continental Shelf Research, v. 25, p. 503–519, https://doi.org/10.1016/j.csr.2004.10.010.

Wan, S., Toucanne, S., Clift, P.D., Zhao, D., Bayon, G., Yu, Z., Cai, G., Yin, X., Révillon, S., Wang, D., Li, A., and Li, T., 2015, Human impact overwhelms long-term climate control of weathering and erosion in southwest China: Geology, v. 43, p. 439–442, https://doi.org/10.1130/G36570.1.

Wang, P., Li, Q., and Li, C.F., 2014, Sedimentology, *in* Wang, P., Li, Q., and Li, C.F., eds., Geology of the China Seas: Amsterdam, Netherlands, Elsevier, Developments in Marine Geology 6, p. 183–340, https://doi.org/10.1016/B978-0-444-59388-7.00004-4.

Xie, X., Müller, R.D., Ren, J., Jiang, T., and Zhang, C., 2008, Stratigraphic architecture and evolution of the continental slope system in offshore Hainan, northern South China Sea: Marine Geology, v. 247, p. 129–144, https://doi.org/10.1016/j.margeo.2007.08.005.

Zhao, R., Chen, S., Olariu, C., Steel, R., Zhang, J.Y., and Wang, H., 2019, A model for oblique accretion on the South China Sea margin: Red River (Song Hong) sediment transport into Qiongdongnan Basin since Upper Miocene: Marine Geology, v. 416, https://doi.org/10.1016/j.margeo.2019.106001.

Zhao, Z., Sun, Z., Sun, L., Wang, Z., and Sun, Z., 2018, Cenozoic tectonic subsidence in the Qiongdongnan Basin, northern South China Sea: Basin Research, v. 30, p. 269–288, https://doi.org/10.1111/bre.12220.

Printed in the USA